SUPPORTING INFORMATION

ALLOSTERIC REGULATION AND SUBSTRATE ACTIVATION IN CYTOSOLIC NUCLEOTIDASE II FROM *LEGIONELLA PNEUMOPHILA*

Bharath Srinivasan[‡,1], Farhad Forouhar[§,1], Arpit Shukla[‡], Chethana Sampangi[‡], Sonia Kulkarni[‡], Mariam Abashidze[§], Jayaraman Seetharaman[§], Scott Lew[§], Lei Mao[#], Thomas B. Acton[#], Rong Xiao[#], John K. Everett[#], Gaetano T. Montelione[#], Liang Tong[§,2] and Hemalatha Balaram[‡,3]

From the [‡]Molecular Biology and Genetics Unit, Jawaharlal Nehru Centre for Advanced Scientific Research, Jakkur, Bangalore 560 064, Karnataka, India, and

the[§]Department of Biological Sciences, Northeast Structural Genomics Consortium, Columbia University, New York, NY 10027

the # Center for Advanced Biotechnology and Medicine, Department of Molecular Biology and Biochemistry, Rutgers University,Department of Biochemistry, Robert Wood Johnson Medical School, Northeast Structural Genomics Consortium, Piscataway, NJ 08854.

Running title: *Allostery in cN-II*

SUPPORTING METHODS

Cloning, expression and purification of LpcN-II

The lpg0095 protein corresponds to NESG target LgR1. The full-length *lpg0095* gene from *Legionella pneumophila* (strain Philadelphia 1 / ATCC 33152 / DSM 7513) was cloned into Nde I and Not I sites (5' to 3' respectively) of a pET21d (Novagen) derivative (conferring ampicillin resistance), generating plasmid pLgR1-21. The recombinant protein contains eight non-native residues (LEHHHHHH) at the carboxy terminus. The construct was verified by standard DNA sequence analysis. The expression plasmid was transformed into *Escherichia coli* XL-1 Gold cloning strain for the purpose of routine plasmid isolation and *E. coli* BL21 (DE3) pMgK for expression (The

expression strain contains an additional plasmid conferring kanamycin resistance and genes expressing the tRNAs for rare codons of arginine and isoleucine).The transformed cells were grown in terrific broth with ampicillin (100 μg/ ml) and kanamycin (50 μg/ ml) as selection markers and induced with IPTG at a final concentration of 0.3 mM. Induction was carried out at 17 ºC for 8 hours. The cells were pelleted down at 2600 x g for 20 minutes and were resuspended in 30 ml of lysis buffer (50 mM Tris HCl, pH 7.4, 100 mM NaCl, 2 mM DTT and 10 % glycerol). The cells were lysed using French© pressure cell press (Thermo IEC Inc., USA) and the obtained cell lysate was centrifuged at 12900 x g for 30 min. The supernatant was kept for binding with nickel nitrilotriacetic acid (Ni-NTA) beads (Ni-NTA His-Bind® Resin, Qiagen, USA) for 3 hrs. The beads were washed extensively with 30 ml of wash buffer (lysis buffer containing 15 mM and 20 mM imidazole, respectively). The bound enzyme was eluted with 5 ml of elution buffer (lysis buffer containing 250 mM imidazole). After the elution of the protein from Ni-NTA beads, EDTA was added to a final concentration of 1mM to prevent oxidation by trace nickel contamination. The protein was concentrated to required volume using Macrosep centrifugal devices (Pall Co., USA) with 10 KDa cutoff membrane and loaded onto a Sephacryl 200 (16 mm X 600 mm) size-exclusion column pre-equilibrated with buffer A (50 mM Tris HCl, pH 7.4, 10 % glycerol, 2 mM DTT and 1 mM EDTA). The fractions containing the protein were pooled, concentrated and stored at - 20 °C. SDS-PAGE analysis was performed using standard protocols [1]. Protein concentrations were determined by the method of Bradford [2] with bovine serum albumin (BSA) as a protein standard. The molecular mass of the protein was confirmed by Mass spectrometry, using a MALDI (matrix-assisted laser-desorption ionization) mass spectrometer (Ultraflex II, BruckerDaltonics, Germany). The protein sample for mass determination was dialysed against water, 1μl of protein (2 μg) was mixed with sinapinic acid (0.1 g of sinapinic acid in 0.5 ml of 50 % acetonitrile and 0.1 % trifluoroacetic acid) in 1:1 ratio, spotted on the MALDI target plate and mass spectra were recorded in the positive ion mode. The identity of the protein was further confirmed by Western blot analysis with anti-His antibodies. Recombinant hexa-histidine tagged full-length LpcN-II showed a single band on SDS-polyacrylamide gel corresponding to a molecular mass of 55 kDa (Supplemental Fig. S1A). MALDI-MS

(Supplemental Fig. S1B) and Western blotting with monoclonal anti-histidine antibodies further confirmed the identity of recombinant LpcN-II (Supplemental Fig. S1C).

The production of the selenomethionine labeled LpcN-II (lpg0095) protein was carried out as part of the high-throughput protein production process of the Northeast Structural Genomics Consortium (NESG) [3]. A single isolate was cultured in MJ9 minimal media [4] supplemented with selenomethionine, lysine, phenylalanine, threonine, isoleucine, leucine and valine for the production of selenomethionine-labeled lpg0095 [5]. Initial growth was carried out at 37 °C until the OD_{600} of the culture reached 0.6-0.8. The incubation temperature was then decreased to 17 °C and protein expression was induced by the addition of IPTG (isopropyl-β-D-thiogalactopyranoside) at a final concentration of 1 mM. Following overnight incubation, the cells were harvested by centrifugation.

Selenomethionyl lpg0095 was purified by standard methods. Cell pellets were resuspended in lysis buffer (50 mM NaH_2PO_4 (pH 8.0), 300 mM NaCl, 10 mM imidazole and 5 mM β-mercaptoethanol) and disrupted by sonication. The resulting lysate was clarified by centrifugation at 26,000 × g for 45 min at 4 °C. The supernatant was loaded onto a Ni-NTA column (Qiagen) and eluted in lysis buffer containing 250 mM imidazole. Fractions containing partially purified lpg0095 were pooled and buffer conditions providing mono-disperse samples were optimized by analytical gel filtration detected by static light scattering, as described elsewhere [3]. Preparative gel filtration (Superdex 75, GE Healthcare) was then performed using a buffer containing 10 mM Tris (pH 7.5), 100 mM NaCl, 5 mM DTT, and 0.02% NaN_3. The purified lpg0095 protein was concentrated to 9.3 mg/ml, flash frozen in aliquots, and used for crystallization screening. Sample purity (>95%) and molecular weight were verified by SDS-PAGE and MALDI-TOF mass spectrometry, respectively. The yield of the purified lpg0095 protein was approximately 36 mg/L, respectively.

Analytical gel filtration

The oligomeric status of the wild-type and mutant proteins was probed by size exclusion chromatography on an analytical Superdex 200 column (10 mm X 300 mm) attached to an AKTA Basic HPLC system. The column was equilibrated with Buffer A (50 mM Tris HCl, pH 7.4) and

calibrated using molecular weight standards, Blue dextran (2000 kDa), β-amylase (200 kDa), alcohol dehydrogenase (150 kDa), bovine serum albumin (66 kDa), carbonic anhydrase (29 kDa) and cytochrome c (12.4 kDa). The flow rate was maintained at 0.5 ml min^{-1}. Purified protein (20μM) was loaded on the column and the elution was monitored at 280 nm. The enzyme was eluted with buffers containing 2M NaCl concentration. The native mass was calculated from a plot of the logarithm of the molecular mass versus elution volume from the column. To monitor the susceptibility of the oligomer to salt concentration, protein samples were pre-incubated for 15 min. with 2 M NaCl. The elution buffer also contained 2 M NaCl.

Phosphate estimation by Chen's assay

The assays were carried out under initial velocity conditions were the product formed was less than 5 % of the initial substrate concentration. 100 μl of reaction volume contained 50 mM Tris HCl, pH 7.4, 20 mM $MgCl_2$, and varying concentrations of substrate. The reaction was initiated by addition of 0.15 μM enzyme and allowed to proceed for 5 min. and 30 min. for GMP and IMP, respectively at 37 °C. The reaction was quenched by addition of 20 μl of 70 % TCA. The reaction mixture was centrifuged at 9500 x g for 10 min. and the supernatant was added to 1 ml of Chen's reagent (6 N sulfuric acid, distilled water, 2.5 % ammonium molybdate and 10 % ascorbic acid mixed in 1:2:1:1 ratio). The reaction mix was allowed to incubate at 37 °C for 30 min. for color stabilization. The absorbance was recorded at 820 nm (molar extinction coefficient is 25000 M^{-1} cm^{-1}) with a double beam Hitachi U-2010 UV-Vis spectrophotometer (Hitachi High Technologies America, Inc., San Jose, CA, USA). Specific activity was defined as μmoles of product formed in one minute by a milligram of enzyme.

To determine the K_m for GMP and dGMP, the respective substrates were titrated and the resultant velocities were plotted against substrate concentration. The data were fit to Hill equation (1)

$$v = \frac{V_{max} \times S^h}{K_m{}^h + S^h} \quad (1)$$

where*v* is the velocity, V_{max} is the maximum velocity, [S] is the substrate concentration, K_m is the Michaelis-Menten constant for GMP (commonly referred to as $[S]_{0.5}$ i.e., substrate concentration at half maximal velocity) and h is the Hill coefficient.

Activity measurements using pNPP as substrate

Assays were initiated with the addition of enzyme to the sample cuvette after zeroing the absorbance reading with respect to the reference cuvette. The rate of p-nitrophenyl phosphate (pNPP) (Fluka/BioChemika, UK) hydrolysis was determined by monitoring the increase in absorbance at 405 nm (molar extinction coefficient (ε) of p-nitrophenol is 18,000 M^{-1} cm^{-1}) at 27 °C. The reaction was monitored continuously for 15-20 minutes. The initial velocities were measured for reaction mixtures containing 30 mM $MgCl_2$. Specific activity was defined as nmol of product formed in one minute by a milligram of enzyme.

To determine the K_m for pNPP, the substrate was titrated at fixed saturating concentration of Mg^{2+} (30 mM) and the resultant velocities were plotted against substrate concentration and fitted to the equation for one-site binding hyperbola (equation 2). The concentration of enzyme used was 5.85 μM. Assuming Mg^{2+} to be a pseudo-substrate, its dissociation constant was determined by titrating Mg^{2+} at saturating concentration of pNPP (15 mM). The data were fit to equation (2).

$$v = \frac{V_{max} \times S}{K_m + S} \qquad (2)$$

where v is the velocity of the enzyme, V_{max} is the maximum velocity, [S] is the substrate concentration, K_m is the Michaelis-Menten constant for pNPP.

Unless mentioned otherwise, all the data were fitted using linear regression and non-linear curve fitting subroutines of GraphPad Prism, version 4.0 (GraphPad Software, Inc., San Diego, CA).

Determination of the dissociation constant (K_D) of [Activator-Mg^{2+}] complexes of LpcN-II

(a)Kinetic Method to determine GTP-Mg^{2+}'s affinity for the enzyme

K_A (Activation constant) values of GTP-Mg^{2+}, dGTP-Mg^{2+} and GDP-Mg^{2+} enzyme complexes were determined at 15 mM pNPP, 0.366 μM enzyme, 30 mM $MgCl_2$ (free) at 27 °C. GTP-Mg^{2+},

dGTP-Mg^{2+} and GDP-Mg^{2+} were titrated from 0.25 mM to 20 mM at fixed concentration of 15 mM pNPP. Corrections were done, to account for the depletion of $MgCl_2$ through chelation with GTP, dGTP and GDP, by taking the dissociation constant for Mg^{2+}-nucleotide complex as 0.353 mM for GTP and dGTP, and 0.820 mM for GDP[6].

Mg^{2+} (free) was computed using equation (3) and the respective dissociation constants as follows.

$$K_D = \frac{[Nucleotide(f)] \times [\mathrm{Mg(f)}]}{[Nucleotide\text{-}Mg\ complex]} \quad (3)$$

Assuming Nucleotide-Mg to be x

$$K_D = \frac{[Nucleotide(t) - x] \times [Mg(t) - x]}{x}$$

where 't' and 'f' are total and free, respectively.

Substituting for nucleotide(t), Mg(t) and the dissociation constant for Mg-nucleotide complex, a quadratic equation is obtained, the solution of which provides the concentration of nucleotide-Mg^{2+} complex.

The experimental points of specific activity at different GTP/dGTP/GDP concentrations and fixed pNPP concentration were fitted to the equation for one-site binding hyperbola (equation (2)) using GraphPad Prism, Version 4 to obtain K_A values for the nucleotide-enzyme complexes.

(b) Equilibrium binding methods to determine GTP-Mg^{2+}'s affinity for the enzyme

GTP-Mg^{2+} dissociation constant for LpcN-II was also determined by equilibrium binding method. 10 µl of cold GTP (200 mM) was diluted with 10 µl ^{32}P-GTP resulting in a final concentration of 100 mM cold GTP with a specific activity of 50 µCi µmol^{-1}. The assay buffer (50 mM Tris HCl, pH 7.4, 30 mM $MgCl_2$, and 0.027 µM of enzyme) was aliquoted into vials containing serially diluted GTP in a total volume of 20 µl. A control with no GTP was maintained. The samples were exposed to UV light (254 nm) (Superfit India Pvt. Ltd.) at a distance of 5 inches (approximate flux of 3- 9 J/m^2) for 20 min at 4 °C. After exposure, the reaction mixture was washed twice with 10 µl of 70 % TCA (containing 100 mM cold GTP to remove non-specifically bound hot GTP) by incubating at 4 °C for 20 min. A

third wash with 80 % cold acetone was given. After each wash step, the samples were centrifuged at 13,000 rpm for 15 min. The pelleted protein was dried till traces of acetone were completely evaporated. The dried pellets were resuspended in SDS-PAGE loading buffer, boiled for 5 min. and loaded on 12 % SDS polyacrylamide gel. The gel was destained, dried and exposed to x-ray film (Kodak, USA) overnight. The exposed film was read using Phosphorimager (Fujifilm, Tokyo, Japan). The radioactive intensity data, normalized for the intensity of the protein band in the Coomassie stained gel, was plotted as a function of GTP concentration and the data points were fit to equation (2) to derive binding parameters.

Screening for activators of LpcN-II activity

Metabolites and Metals that were checked for their ability to activate LpcN-II were fructose-1,6-bisphosphate(1 mM, 15 mM pNPP), adenosine triphosphate (2.5 mM at 15 mMpNPP), deoxyadenosinetriphosphate (2.5 mM at 15 mM pNPP), adenosine diphosphate (0.5, 1, 2.5 mM at 15 mM pNPP), adenosine 5'-[γ-thio] triphosphate (100μM at 15 mM pNPP), diadenosinetetraphosphate (100 and 500 μM at pNPP concentrations of 1 mM and 10 mM), diadenosinetriphosphate (100 and 500 μM at pNPP concentrations of 1 mM and 10 mM), diadenosinepentaphosphate (2.5 mM at 15 mM pNPP), diadensoinehexaphosphate (250 μM at 15 mM pNPP), 2,3-bisphosphoglycerate (1 mM at 10 mM pNPP), Potassium chloride, Sodium chloride, orthovanadate (100 μM and 250 μM at 15 mM pNPP), pervanadate(50 μM and 100 μM at 15 mM pNPP), uridinetriphosphate (2.5 mM at 15 mM pNPP),cytosine triphosphate (2.5 mM at 15 mM pNPP), deoxycytosinetriphosphate(2.5 mM at 15 mM pNPP), deoxythymidinetriphosphate (2.5 mM at 15 mM pNPP), Adenosine 5′-[β,γ-imido]triphosphate(0.5 mM at 15 mM pNPP), Guanosine 5′-[β,γ-imido]triphosphate (0.5 mM and 1 mM at 15 mM pNPP), 5-phospho D-ribose-1-diphosphate (2.5 mM at 15 mM pNPP), inosine triphosphate (1 mM at 15 mM pNPP), glucose-6-phosphate (1 mM at 15 mM pNPP) and guanosine (5 mM at 15 mM pNPP). All the assays were done at 27 °C, 30 mM Mg^{2+} (total) and 50 mM Tris HCl, pH 8.0. All assays had 3.66 μM enzyme.

Synthesis of orthovanadate, decavanadate and pervanadate was carried out as follows. Decavanadate-free solutions were obtained by dissolving orthovanadate at a concentration of 200 mM

in distilled water. Final dilutions of the assay solution were not followed by an adjustment of the pH in order to avoid the formation of decavanadate [7]. The alkalinity of the vanadate was not disturbing, because of its very low final concentrations in the assay medium (μM concentrations). Decavanadate was synthesized as specified by Varga*et al.*[8] with minor modifications. Briefly, decavanadate solutions were prepared by adjusting the pH of a 200 mM Na_3VO_4 solution to 2.0; acid pH favors the accumulation of orange-yellow decavanadate species. After 6-12 hours incubation at 4 °C, the pH was adjusted to 7.4 at 4 °C and the solution was used immediately for experiments. The activation of LpcN-II by decavanadate was tested at 10 nM to 1000 nM, respectively. Pervanadate was synthesized as specified in Huyer*et al.* [9]. Briefly, Pervanadate stock solution (1 mM) was prepared by adding 10 μl of 100 mM vanadate and 50 μl of 100 mM hydrogen peroxide (diluted from a 30 % stock in 20 mM HEPES, pH 7.3) to 940 μl of H_2O. Excess hydrogen peroxide was removed by adding catalase (100 μg/ml final concentration = 260 units/ml) 5 min after mixing the vanadate and hydrogen peroxide. The pervanadate solutions were used within 5 min to minimize decomposition of the vanadate-hydrogen peroxide complex.

Activation of pNPP hydrolysis by GTP

Activation of pNPP hydrolysis by GTP was monitored by performing activation kinetics wherein pNPP was titrated at various fixed concentrations of GTP and vice versa. The assay condition for pNPP titration at various fixed GTP concentrations was 50 mM Tris HCl, pH 8.0, and 30 mM $MgCl_2$ (free) at 27 °C in a total reaction volume of 250 μl. Depletion of Mg^{2+} by GTP was corrected by using the dissociation constant of Mg^{2+}-GTP [6] .As at higher GTP concentrations the rates of reaction were greatly enhanced, the enzyme concentration was varied as follows, 3.66 μM at 0.05 mM GTP, 1.46 μM at 0.1 mM and 0.25 mM GTP, 0.73 μM at 0.5 mM GTP, 0.37 μM at 1mM, 2mM and 5mM GTP and 0.18 μM at 7 mM GTP, respectively. Each point was done in triplicate. The temperature of the reaction mix was maintained at 27 °C by using a water bath attached to a water-circulated cell holder.

Mg^{2+} depletion due to pNPP chelation was ignored because of the high dissociation constant for Mg-pNPP complex (5.88 mM) [10] and because of the presence of saturating magnesium (greater than 10 times the K_m value of Mg^{2+} for the enzyme).

The assay condition, for GTP titration at various fixed pNPP concentrations, was 50 mM Tris HCl, pH 8.0, 30 mM $MgCl_2$ (free) and 1.83 μM of enzyme at 27 °C in a total reaction volume of 250 μL. $MgCl_2$ was constantly varied as GTP was titrated along the curve to maintain a constant 30 mM concentration of free Mg^{2+}. The various pNPP concentrations were 0.5 mM, 0.75 mM, 1 mM, 1.5 mM and 2 mM, respectively. Each point was done in duplicate. The curve fitting was done using GraphPad Prism, version 4 by considering each replicate Y value as an individual point.

Effect of guanosine on activation of pNPP hydrolysis by GTP

Effect of guanosine on GTP activation of pNPP hydrolysis was performed by monitoring pNPP hydrolysis in the presence of GTP and guanosine. The assay conditions were 50 mM Tris pH 8.0, 30 mM $MgCl_2$, 5mM Guanosine and 2mM GTP. As guanosine was prepared in 0.1N NaOH, control reactions in the absence of guanosine also contained an equivalent amount of alkali. The assay was performed in triplicate and the result was subjected to paired t-test. '*' indicates $p<0.05$.

Activation of GMP hydrolysis by GTP

Activation of GMP hydrolysis by GTP was monitored by ion-pair reverse phase high performance liquid chromatography (IP-RP-HPLC). The ion-pairing agent used for the studies was tetrabutylammonium hydrogen sulphate (TBAHS). Tetrabutylammonium is a positively charged ion-coupling agent neutralizing the negative charge on phosphates. The column (Sephasil peptide C-18, 5μ, ST 4.6/250, Amersham Pharmacia) was equilibrated with solution A (2 mM TBAHS), the sample injected and a step gradient (25 % B in 1 column volume, 33 % B in 3 column volume and 95 % B in 2 column volume) of solution B (100 % methanol with 2 mM TBAHS) was applied with a flow rate of 0.3 ml/min. Standards comprising of guanosine, GMP and GTP (individually and in combination) were run to ascertain the volumes at which they eluted and their identity was established using MALDI-mass spectrometry. The reaction was carried out in 50 mM Tris HCl, pH 7.4, 30 mM $MgCl_2$ and the substrate concentration was 1.5 mM GMP in a final volume of 100 μl. The reaction was initiated by addition of 0.29 μM enzyme, incubated for 5 min. at 37 °C and quenched by addition of 100 mM EDTA followed by boiling for 5 minutes. The boiled sample was centrifuged and the supernatant was injected into the column. The elution of guanosine, GMP and GTP was measured at 254 nm and the concentration estimated by calculating the area under the curve.

Activation of GMP hydrolysis by GTP was also monitored by Chen's assay, where GMP was titrated at several fixed GTP concentrations. The concentrations of GTP used were 0 mM, 0.25 mM, 0.5 mM, 1 mM and 5mM. The data were fit to the Hill's equation with the non-linear curve fitting algorithms of GraphPad Prism version 4.0.

Crystallization and data collection.

Selenomethionyl lpg0095 (native cN-II) was crystallized in SO_4-, and PO_4-bound forms by vapor diffusion, hanging-drop method at 20 °C. Two μl of protein solution containing lpg0095 (9.3 mg/ml, in 10 mM Tris-HCl, pH 7.5, 100 mM NaCl, 5 mM DTT, and 0.02 % NaN_3) were mixed with 2 μl of the precipitant solution consisting of 100 mM MES, pH 6.15, 20 % (w/v) PEG400, and 100 mMKBr for crystallization of the SO_4-bound crystals. The crystals of the PO_4-bound complex were obtained using the same procedure as that of the SO_4-bound one, except 5 mM phosphate ion was added into protein solution prior to crystallization. Crystals of selenomethionyl lpg0095 belong to space group $I4_122$ for SO_4-, PO_4-bound enzyme. There is one molecule of lpg0095 in the crystallographic asymmetric unit of SO_4- and PO_4-bound structures. For the SO_4-boundselenomethionyl lpg0095, multiple-wavelength anomalous diffraction (MAD) data sets to resolution 2.9 Å were collected at the peak, edge, and remote absorption wavelengths of selenium at the X4A beamline of the National Synchrotron Light Source (NSLS).

Attempts to obtain diffraction-quality crystals of ligand-bound enzyme by soaking crystals of the uncomplexed enzyme in saturated solutions of the various guanine nucleotides were unsuccessful owing to crystal breakage or poor diffraction. Conditions for the crystallization of nucleotide-complexed protein were obtained by screening all the conditions of Hampton crystal screen 1, crystal screen 2, Index screen 1, Index screen 2, SaltRX and PEG/Ion screen (Hampton Reasearch, USA). In the initial attempts to obtain nucleotide complexed LpcN-II crystal, GTP was used in the crystallization screens. The protein was preincubated with 20 mM of GTP, 5 mM $MgCl_2$ and 5 mM DTT. for 3 hours at 4 °C prior to crystallization. Supplemental Table S4 summarizes the various conditions under which the GTP-complexed protein crystallized. These crystals yielded low resolution diffraction data. Thereafter, GMP, GDP, dGDP, GMP-PCP, GMP-PNP were included in

subsequent crystallization attempts and screens were set around the conditions listed in Table S4. Crystals obtained from solutions of LpcN-II preincubated with GMP-PNP diffracted to good resolution. These crystals were obtained using crystal screen II, condition 78 (0.1 M Bis-Tris HCl, pH 5.5, 0.2M ammonium acetate, 25 % w/v PEG3350). The crystals prior to mounting were pre-incubated in a solution containing10 mM GMP-PNP, 5 mM $MgCl_2$ and 20 % (v/v) ethylene glycol in the reservoir buffer.

The monoclinic data for the GMP-PNP-complexed crystal was collected at a wavelength of 1.5418 Å on a Rigaku RU-200 rotating-anode X-ray generator equipped with a 300 µm focal cup. The images were recorded using a MAR 345 image-plate detector. Data sets were collected at 100 K from a single crystal mounted on a cryo loop to a resolution of 2.53Å. 200 frames were acquired and all frames were used for data processing. The crystal form belonged to monoclinic space group *C*2. The volume of the asymmetric unit in this crystal form was compatible with four subunits of cN-II. Matthews coefficient (V_M) and solvent content of the crystal were 2.65 $Å^3Da^{-1}$ and 58.57 % (v/v), respectively. Data sets were processed and scaled using *DENZO* and *SCALEPACK* of the *HKL* suite [11].

References

1. Laemmli, U. K. (1970) Cleavage of structural proteins during the assembly of the head of bacteriophage T4, *Nature.* **227**, 680-5.
2. Bradford, M. M. (1976) A rapid and sensitive method for the quantitation of microgram quantities of protein utilizing the principle of protein-dye binding, *Analytical biochemistry.* **72**, 248-54.
3. Acton, T. B., Gunsalus, K., Xiao, R., Ma, L., Aramini, J., Baron, M. C., Chiang, Y., Clement, T., Cooper, B., Denissova, N., Douglas, S., Everett, J. K., Palacios, D., Paranji, R. H., Shastry, R., Wu, M., Ho, C.-H., Shih, L., Swapna, G. V. T., Wilson, M., Gerstein, M., Inouye, M., Hunt, J. F. & Montelione, G. T. (2005) Robotic cloning and protein production platform of the Northeast Structural Genomics Consortium, *Methods Enzymol.* **394**, 210-243.
4. Jansson, M., Li, Y.-C., Jendeberg, L., Anderson, S., Montelione, G. T. & Nilsson, B. (1996) High level production of uniformly 15N- and 13C-enriched fusion proteins in Escherichia coli, *J Biomol NMR.* **7**, 131-141.
5. Doublie, S., Kapp, U., Aberg, A., Brown, K., Strub, K. & Cusack, S. (1996) Crystallization and preliminary X-ray analysis of the 9 kDa protein of the mouse signal recognition particle and the selenomethionyl-SRP9, *FEBS Lett.* **384**, 219-221.
6. Smith, R. M. & Alberty, R. A. (1956) The apparent stability constants of ionic complexes of various adenosine phosphates and divalent cations. , *Journal of American Chemical Society.* **78**, 2376-2380.
7. Kadota, S., Fantus, I. G., Deragon, G., Guyda, H. J., Hersh, B. & Posner, B. I. (1987) Peroxide(s) of vanadium: a novel and potent insulin-mimetic agent which activates the insulin receptor kinase, *Biochemical and biophysical research communications.* **147**, 259-66.

8. Varga, S., Csermely, P. & Martonosi, A. (1985) The binding of vanadium (V) oligoanions to sarcoplasmic reticulum, *European journal of biochemistry / FEBS.* **148**, 119-26.
9. Huyer, G., Liu, S., Kelly, J., Moffat, J., Payette, P., Kennedy, B., Tsaprailis, G., Gresser, M. J. & Ramachandran, C. (1997) Mechanism of inhibition of protein-tyrosine phosphatases by vanadate and pervanadate, *The Journal of biological chemistry.* **272**, 843-51.
10. Kashiwamata, S., Goto, S., Semba, R. K. & Suzuki, F. N. (1979) Inhibition by bilirubin of (Na+ + K+)-activated adenosine triphosphatase and K+-activated p-nitrophenylphosphatase activities of NaI-treated microsomes from young rat cerebrum, *The Journal of biological chemistry.* **254**, 4577-84.
11. Otwinowski, Z. & Minor, W. (1997) Processing of X-ray diffraction data collected in oscillation mode, *Methods in enzymology.* **276**, 307-326.
12. van den Berghe, G., van Pottelsberghe, C. & Hers, H. G. (1977) A kinetic study of the soluble 5'-nucleotidase of rat liver, *The Biochemical journal.* **162**, 611-6.
13. Itoh, R. (1982) Studies on some molecular properties of cytosol 5'-nucleotidase from rat liver, *Biochimica et biophysica acta.* **716**, 110-3.
14. Allegrini, S., Scaloni, A., Careddu, M. G., Cuccu, G., D'Ambrosio, C., Pesi, R., Camici, M., Ferrara, L. & Tozzi, M. G. (2004) Mechanistic studies on bovine cytosolic 5'-nucleotidase II, an enzyme belonging to the HAD superfamily, *European journal of biochemistry / FEBS.* **271**, 4881-91.
15. Spychala, J., Chen, V., Oka, J. & Mitchell, B. S. (1999) ATP and phosphate reciprocally affect subunit association of human recombinant High Km 5'-nucleotidase. Role for the C-terminal polyglutamic acid tract in subunit association and catalytic activity, *European journal of biochemistry / FEBS.* **259**, 851-8.
16. Marques, A. F., Teixeira, N. A., Gambaretto, C., Sillero, A. & Sillero, M. A. (1998) IMP-GMP 5'-nucleotidase from rat brain: activation by polyphosphates, *Journal of neurochemistry.* **71**, 1241-50.
17. Pesi, R., Turriani, M., Allegrini, S., Scolozzi, C., Camici, M., Ipata, P. L. & Tozzi, M. G. (1994) The bifunctional cytosolic 5'-nucleotidase: regulation of the phosphotransferase and nucleotidase activities, *Archives of biochemistry and biophysics.* **312**, 75-80.
18. Bontemps, F., Van den Berghe, G. & Hers, H. G. (1988) 5'-Nucleotidase activities in human erythrocytes. Identification of a purine 5'-nucleotidase stimulated by ATP and glycerate 2,3-bisphosphate, *The Biochemical journal.* **250**, 687-96.
19. Pinto, R. M., Canales, J., Gunther Sillero, M. A. & Sillero, A. (1986) Diadenosine tetraphosphate activates cytosol 5'-nucleotidase, *Biochemical and biophysical research communications.* **138**, 261-7.
20. Spychala, J., Madrid-Marina, V. & Fox, I. H. (1988) High Km soluble 5'-nucleotidase from human placenta. Properties and allosteric regulation by IMP and ATP, *The Journal of biological chemistry.* **263**, 18759-65.
21. Le Hir, M. (1991) A soluble 5'-nucleotidase in rat kidney. Stimulation by decavanadate, *The Biochemical journal.* **273 (Pt 3)**, 795-8.
22. Bretonnet, A. S., Jordheim, L. P., Dumontet, C. & Lancelin, J. M. (2005) Regulation and activity of cytosolic 5'-nucleotidase II. A bifunctional allosteric enzyme of the Haloacid Dehalogenase superfamily involved in cellular metabolism, *FEBS letters.* **579**, 3363-8.
23. Bontemps, F., Vincent, M. F., Van den Bergh, F., van Waeg, G. & Van den Berghe, G. (1989) Stimulation by glycerate 2,3-bisphosphate: a common property of cytosolic IMP-GMP 5'-nucleotidase in rat and human tissues, *Biochimica et biophysica acta.* **997**, 131-4.
24. Bianchi, V. & Spychala, J. (2003) Mammalian 5'-nucleotidases, *The Journal of biological chemistry.* **278**, 46195-8.
25. Notredame, C., Higgins, D. G. & Heringa, J. (2000) T-Coffee: A novel method for fast and accurate multiple sequence alignment, *Journal of molecular biology.* **302**, 205-17.
26. Kumar, S., Tamura, K. & Nei, M. (2004) MEGA3: Integrated software for Molecular Evolutionary Genetics Analysis and sequence alignment, *Briefings in bioinformatics.* **5**, 150-63.
27. Gouet, P., Courcelle, E., Stuart, D. I. & Metoz, F. (1999) ESPript: analysis of multiple sequence alignments in PostScript, *Bioinformatics.* **15**, 305-8.

Table S1. Ligand screen to determine the substrate/s and cofactor/s for LpcN-II.

S. No	Substrate and cofactor	Specific activity (nmol min^{-1} mg^{-1})
1	GMP[1, 3,7]	3990 ± 117
2	dGMP[1, 3,7]	390 ± 23
3	IMP[1,3,7]	95 ± 11
4	AMP[1,3,7]	20 ± 5
5	XMP[1,3,7]	14 ± 3
6	UMP[1,3,7]	11 ± 2
7	CMP[1,3,7]	41 ± 3
8	pNPP[1,5, 4]	0.5 ± 0.1
9	chloro acetic acid[2,6]	NA
10	2-chloro ethanol[2,6]	NA
11	p-chloro aniline[2,6]	NA
12	Magnesium chloride[4,5]	0.85 ±0.02
13	Manganese chloride[4,5]	0.29 ± 0.02
14	Calcium chloride[4,5]	NA
15	Cobalt chloride[4,5]	NA
16	Nickel chloride[4,5]	NA
17	Copper chloride[4,5]	NA

Footnotes: [1]The cofactor used was 30 mM $MgCl_2$, [2]The cofactor used was 30 mM magnesium acetate, [3]The buffer used was 50 mM Tris HCl, pH 7.4, [4]The substrate used was 15 mM pNPP, [5]The buffer used was Tris HCl, pH 8.0, [6]The buffer used was Tris acetate, pH. 8.0. [7]The concentration of nucleoside monophosphate was 5 mM, NA**,** no activity.

Table S2. Summary of kinetic parameters of LpcN-II and cN-IIs from various organisms. n_H represents the Hill coefficient.

Source	IMP			GMP			AMP		
	$S_{0.5}$ mM	V_{max} μmol min^1 mg^{-1}	n_H	$S_{0.5}$ mM	V_{max} μmol min^1 mg^{-1}	n_H	$S_{0.5}$ mM	V_{max} μmol min^1 mg^{-1}	n_H
Rat Liver[1,2]	1.2[1], 0.2[2]	0.025[1], NR[2]	1.1[1], NR[2]	NR[1]	0.038[1]	1.1[1]	10[1], 8.7[2]	0.019[1], NR[2]	1.6[1], NR[2]
Bovine cN-II[3]	0.1±0.04	72(sec^{-1})*	NR	NR	NR	NR	NR	NR	NR
Human r-cN-II[4]	4.1± 0.2	19.3± 1.1	1.2	NR	NR	NR	NR	NR	NR
Rat Brain[5]	0.6	1	0.8	4.6	5	1	15	3	2.3
Calf thymus[6]	0.1	1.5	NR	NR	NR	NR	NR	NR	NR
Human erythrocytes[7]	0.4	~1.5	NR	0.8	~1	NR	NR	NR	NR
Artemia embryos[8]	2.8	1	1	3.5	1.2	1	21	1	1.9
Human Placenta[9]	0.3± 0.1	0.4±0.0	1.3	NR	NR	NR	NR	NR	NR
Rat Kidney [10]	>1	~ 0.5	NR	NR	NR	NR	NR	NR	NR
LpcN-II[√]	18 ± 9[a] 118 ± 10[a]	0.4 ± 0.1[b] 1.3 ±0.2[b]	----	7.2±0.3	11.1±0.2	2.1± 0.2	ND	ND	ND

Footnotes. *k_{cat} , [√]This study, [1][12], [2][13], [3][14], [4][15], [5][16], [6][17], [7][18], [8][19], [9][20], [10][21]. **ND,** Not determinable, **NR,** Not reported, [a]Lower and higher K_m values from biphasic curves. [b]Lower and higher V_{max} values from biphasic curves. The parameters were derived from extrapolation of intercepts from Eadie-Hofstee plot.

Table S3. Screening for activators of LpcN-II activity. 15 mM pNPP was used as substrate in the assays. The reaction mixture contained 50 mM Tris HCl, pH 8.0, 30 mM $MgCl_2$. The concentrations of ligands used in the screen are as mentioned in Supplemental Methods.

		Activation/ No activation	
No.	Activator screen	LpcN-II	Human cN-II
1	NaCl	No activation	Activation[1]
2	KCl	No activation	Activation[1]
3	Orthovanadate	Inhibition	Activation
4	Pervanadate	No activation	Activation
5	Decavanadate	No activation	Activation[2]
6.	Inorganic Phosphate	Inhibition[7]	NA
7	Inorganic pyrophosphate	No activation	NA
8	Fructose1,6 bisphosphate	No activation	NA
9	Glucose-6-phosphate	No activation	NA
10	5-Phosphoribosyl pyrophosphate	No activation	NA
11	2,3-BPG	No activation	Activation[3]
12	AP_3A	No activation	NA
13	AP_4A	No activation	Activation[4]
14	AP_5A	No activation	Activation[4]
15	AP_6A	No activation	Activation[4]
16	ATP	No activation	Activation[5]
17	dATP	No activation	Activation
18	ADP	No activation	Activation[6]
19	AMP-PNP	No activation	NA
20	ATP-γ-S-Li_4	No activation	NA
21	UTP	No activation	NA
22	CTP	No activation	NA
23	dCTP	No activation	NA
24	dTTP	No activation	NA
25	GTP	Potent Activation[7]	NA
26	dGTP	Potent Activation[7]	NA

27	GDP	Potent Activation[7]	NA
28	GMP-PNP	Potent Activation[7]	NA
29	AMP	No activation	NA
30	GMP	Activation	NA
31	XMP	No activation	NA
32	IMP	No activation	NA
33	ITP	No activation	NA
34	cAMP	No activation	NA
35	cGMP	No activation	NA
36	UMP	No activation	NA
37	CMP	No activation	NA
38	ddATP	No activation	NA
39	ddGTP	Potent activation	NA
40	ddCTP	No activation	NA
41	Adenosine	No activation	NA
42	Guanosine	Weak activation	NA
43	Xanthosine	No activation	NA

Footnotes. NA, Not Applicable, [1][22], [2][21], [3][23], [4][19], [5][24], [6][14], [7]this study.

Table S4. Kinetic parameters of the LpcN-II enzyme for the substrates, pNPP and GMP in the presence and absence of activator GTP.

substrate	No activator					Activator (GTP[a])		
	$K_m/S_{0.5}$[b] (mM)	V_{max} (μmol min^{-1} mg^{-1})	k_{cat} (sec^{-1})	$k_{cat}/S_{0.5}$ (sec^{-1} mM^{-1})	n_H	$K_m/S_{0.5}$[b] (mM)	V_{max} (μmol min^{-1} mg^{-1})	n_H
pNPP	5.1 ± 0.9	1.0 ± 0.1*	1.0×10^{-3}	0.1×10^{-3}	1	4.4 ± 0.6	134 ± 6*	1
GMP	7.2 ± 0.3	13.2 ± 0.4	12.4	1.7	2.1 ± 0.2	5.1 ± 0.3	8.1 ± 0.3	1.2 ± 0.2

**Footnotes. ***nmol min^{-1} mg^{-1}, [a]5 mM and 20 mM GTP were used in GMP and pNPP assays respectively. [b] Either $S_{0.5}$ or K_m is used depending on the kinetic profile.

Table S5. Summary of conditions under which the GMP-PNP-liganded LpcN-II was crystallized.

S.No	Crystallization condition	Hampton screen no.
1.	0.1M Bicine pH 9.0, 2% w/v Dioxane, 10% w/v PEG 20,000	Crystal screen II, 48
2.	0.1M Bis-Tris pH 5.5, 0.2M ammonium acetate, 25% w/v PEG3350	Index screen II, 78
3.	0.1M Bis-Tris pH 5.5, 0.2M magnesium chloride hexahydrate, 25% w/v PEG3350	Index screen II, 82
4.	0.1M Bis-Tris pH 5.5, 0.2M Lithium Sulfate monohydrate, 25% w/v PEG3350	Index screen II, 74
5.	0.1M Hepes pH 7.0, 30% v/v Jeffamine ED2001	Index screen I, 39

Legend to Supplemental Figures

Figure S1. Purification and characterization of LpcN-II.**(A)** SDS-PAGE of purified LpcN-II. **(B)** MALDI-MS of LpcN-II. The protein gave an average molecular mass of 54,633 Da with the expected theoretical mass being 54,657 Da. **(C)** Western blot confirmation of the identity of the protein. Monoclonal anti-histidine antibody (Sigma-Aldrich Co., USA) was used as probe. **(D)** Analytical gel filtration profile of LpcN-II. Inset shows the standard curve obtained with protein molecular weight standards (Sigma-Aldrich Co., USA) ALDH- alcohol dehydrogenase, BSA- bovine serum albumin. The protein elutes at a volume corresponding to that of a tetramer (220 kDa). The observation was further confirmed by dynamic light scattering measurements (data not shown). Presence of high salt (2 M NaCl) or varying the protein concentration did not alter the oligomeric state of the protein (data not shown).

Figure S2. GTP binding and activation of LpcN-II. **(A)**Determination of dissociation constant for GTP-Mg^{2+} undercatalytic condition wherein GTP-Mg^{2+} was titrated at a fixed concentration of pNPP (15 mM). **(B)**Determination of dissociation constant for GTP-Mg^{2+} underequilibrium conditions by titrating [GTP] at fixed LpcN-II concentration of 0.027 μM. Radiolabeled ^{32}P-GTP of specific activity 50 μCi/μmol was used. The samples were UV cross-linked by exposing to UV light (254 nm) (Superfit India Pvt. Ltd.) at a distance of 5 inches (approximate flux of 3- 9 J/m^2) for 20 min at 4 °C.The radioactive intensity data, normalized for the intensity of the protein band in the Coomassie stained gel, was plotted as a function of GTP-Mg^{2+} concentration and the data points were fit to equation (2) to derive binding parameters. **(C)** Activation of pNPP hydrolysis by GTP. The figure shows the double-reciprocal plot where each line corresponds to varying [pNPP] at different fixed concentrations of GTP-Mg^{2+} with $MgCl_2$ (free) kept constant at 30 mM. **(D)** Double-reciprocal plot 1/*v*versus 1/ [GTP-Mg^{2+}] at different fixed concentration of pNPP. Free $MgCl_2$ was kept constant at 30 mM. Corrections for reduction in free [Mg^{2+}] due to formation of GTP-Mg^{2+} complex was done by using a K_D value of 0.353 mM. Data were fitted using GraphPad prism Software, version 4.0 (GraphPad Software, Inc., San Diego, CA).

Figure S3. Modulation of GTP activation by various ligands. **(A)** Effect of GMP on activation of pNPP hydrolysis by GTP. The various lines indicate the time scans of pNPP hydrolysis. **(B)** GMP titration at several fixed GTP-Mg^{2+} concentrations and 15 mM pNPP. Formation of pNP was monitored at 405 nm. It is clearly evident that with increasing GMP, the activation brought by GTP is reduced. **(C)** 1/*v*versus 1/[GTP-Mg^{2+}] plots at different fixed GDP-Mg^{2+} concentrations wherein the hydrolysis of pNPP was monitored. Note that GDP inhibits activation of pNPP hydrolysis by GTP competitively. **(D)** Histogram representing the effect of guanosine on activation of pNPP hydrolysis by GTP. The data pair was subjected to paired t-test. '*' indicates $p<0.05$. **(E)** Titration of GTP-Mg^{2+} at several fixed ITP-Mg^{2+} concentrations. Note that ITP binds to the activator binding site and competitively inhibits activation of pNPP hydrolysis by GTP**. (F)** Titration of GTP-Mg^{2+} at several fixed ATP-Mg^{2+} concentrations. Note that the curves are overlapping indicating that ATP does not reduce GTP activation.

Figure S4. Purification and characterization of LpcN-II mutants. **(A)** SDS-PAGE profile of purified wild-type LpcN-II, Y421S, R86A and Y421S/R86A. The recombinant proteins were purified to homogeneity as is evident from the figure. The identity of each protein is indicated. The numbers indicate the molecular weight of marker proteins in kDa. **(B)** Analytical size-exclusion chromatography of wild-type, Y421S and Y421S/R86A LpcN-II. The protein elutes at a volume corresponding to that of a tetramer. Inset shows the standard curve generated using with proteins of different molecular weights. Adh: alcohol dehydrogenase and BSA: bovine serum albumin.

Figure S5. Active site-allosteric site connectivity.**(A)** Chain of residues connecting the active site to the activator site as deduced from multiple sequence alignment (MSA). The protein is shown in cartoon representation and the chain of residues is indicated as ball and stick representation in yellow coloration with van derwaals surface shown. The motif IV residues Asp303 and His304 are shown as ball and stick representation in blue color. GMP is in CPK representation. The figure was generated with PyMol version 0.99 (DeLano Scientific LLC). (**B)** Segments from MSA of cN-II sequences from various kingdoms of life. Conserved residues are indicated with red blocks and the numbers above the

alignment refers to *Legionella* sequence. The MSA was generated using T-Coffee [25] and the accession numbers of the sequences are as specified in the legend to supplemental Figure S6.

Figure S6. Phylogenetic tree and multiple sequence alignment of cN-IIs from different organisms.**(A)** Phylogenetic tree of cN-II sequences from various kingdoms of life. Clades representing sequences belonging to kingdom animalia, kingdom plantae, kingdom algae and kingdom prokaryotes cluster separately. The sequences were downloaded from NCBI and the accession numbers are as follows: *Ostreococcuslucimarinus* CCE9901 (XP_001420373.1), *Thalassiosirapseudonana* CCMP1335 (XP_002287876.1), *Phaeodactylumtricornutum* CCAP 1055/1(XP_002177186.1), *Chlamydomonasreinhardtii* (XP_001693752.1), *Drosophila melanogaster* (NP_573289.2), *Caenorhabditiselegans* (NP_508491.1), *Daniorerio* (CAM12923.1), *Musmusculus* (AAH64760.1), *Equuscaballus* (XP_001499570.1), Human (2J2C), *Xenopuslaevis* (NP_001086300.1), *Anopheles gambiae* str. PEST (XP_310728.4), *Schistosomamansoni* (XP_002576111.1), *Physcomitrella patens subsp. Patens* (XP_001782705.1), *Oryza sativa* (japonica cultivar-group) (NP_001051421.1), *Zeamays* (NP_001151027.1), *Arabidopsis thaliana* (NP_177657.2), *Ricinuscommunis* (XP_002510387.1), *Vitisvinifera* (CAO70936.1), *Populustrichocarpa* (ABK95470.1), *Legionella drancourtii* LLAP12 (ZP_05110137.1), *Legionella pneumophila str. Corby* (YP_001249459.1), *Legionella pneumophila str. Lens*(YP_125472.1), *Legionella pneumophila str. Paris* (YP_122460.1), *Legionella pneumophila subsp. pneumophila str. Philadelphia* 1(YP_094149.1), *Bdellovibriobacteriovorus* HD100(NP_970282.1), *Haliangiumochraceum* DSM 14365(ZP_03882403.1), *Salinibacterruber* DSM 13855 (YP_446875.1), *Myxococcusxanthus* DK 1622(YP_635204.1), *Sorangiumcellulosum* 'So ce 56'(YP_001614379.1), *Anaeromyxobacter sp.* Fw109-5 (YP_001379156.1), *Myxococcusxanthus* DK 1622 (YP_631895.1), *Anaeromyxobacterdehalogenans* 2CP-1(YP_002492482.1), *Stigmatellaaurantiaca* DW4/3-1(ZP_01466421.1), *Anaeromyxobacter dehalogenans*2CP-1(YP_002492482.1), *Anaeromyxobacter sp. K* (YP_002134347.1), *Sorangiumcellulosum* 'So ce 56' (YP_001614954.1), *Anaeromyxobacterdehalogenans* 2CP-C (YP_465079.1), *Plesiocystispacifica* SIR-1(ZP_01905669.1), *Stigmatellaaurantiaca* DW4/3-1 (ZP_01461256.1). The multiple sequence alignment was generated

by T-Coffee [25] and MEGA 4 was used to generate the phylogenetic tree [26]. **(B)** Multiple sequence alignment (MSA) of cN-II sequences from various organisms highlighting the absence of the carboxy terminal acidic stretch in prokaryotic sequences. The alignments in this panel was generated by T-Coffee [25] and the figures were generated using the web interface of ESpript[27].

Figure S1. Purification and characterization of LpcN-II.

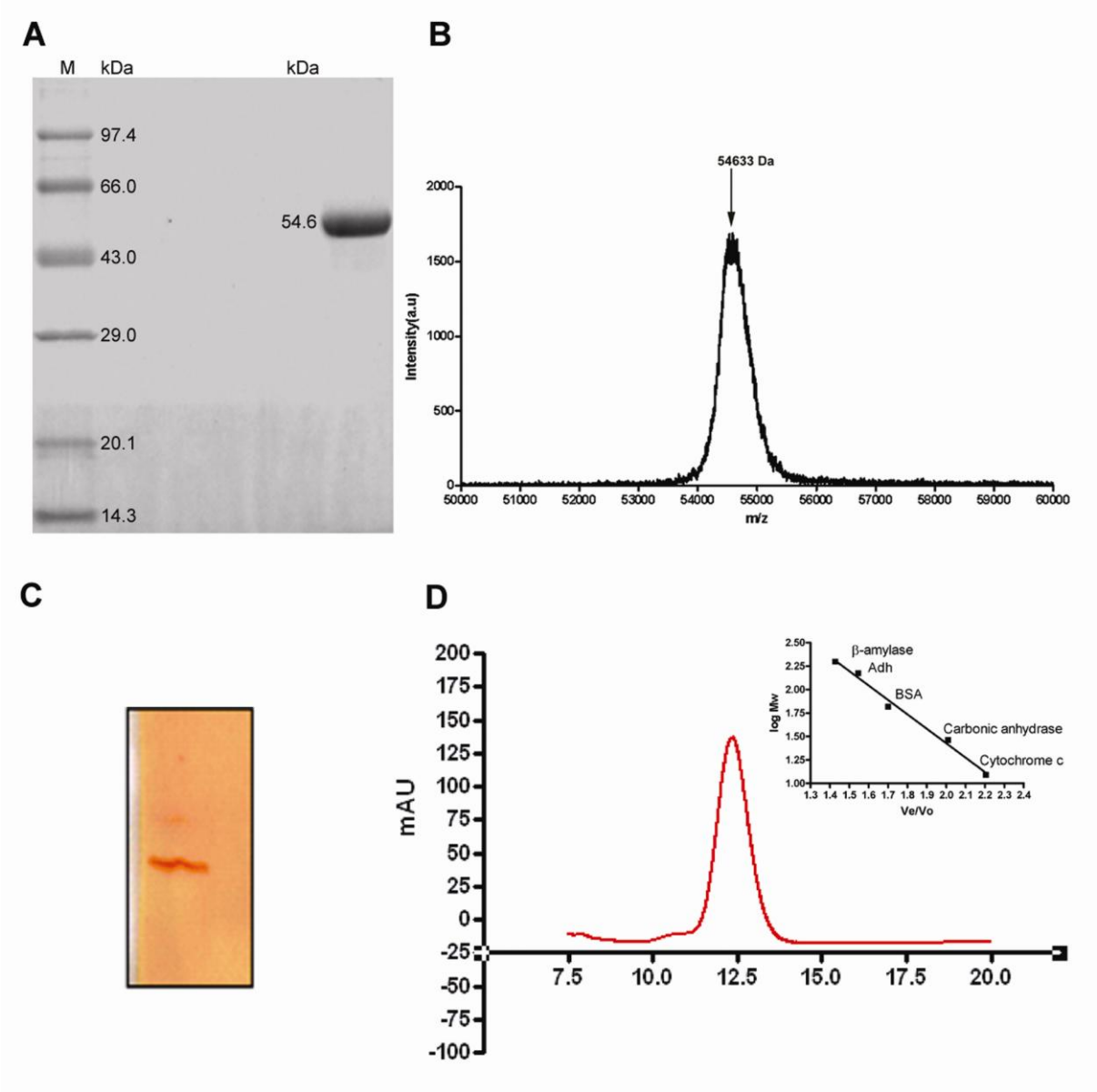

Figure S2. GTP binding and activation of LpcN-II.

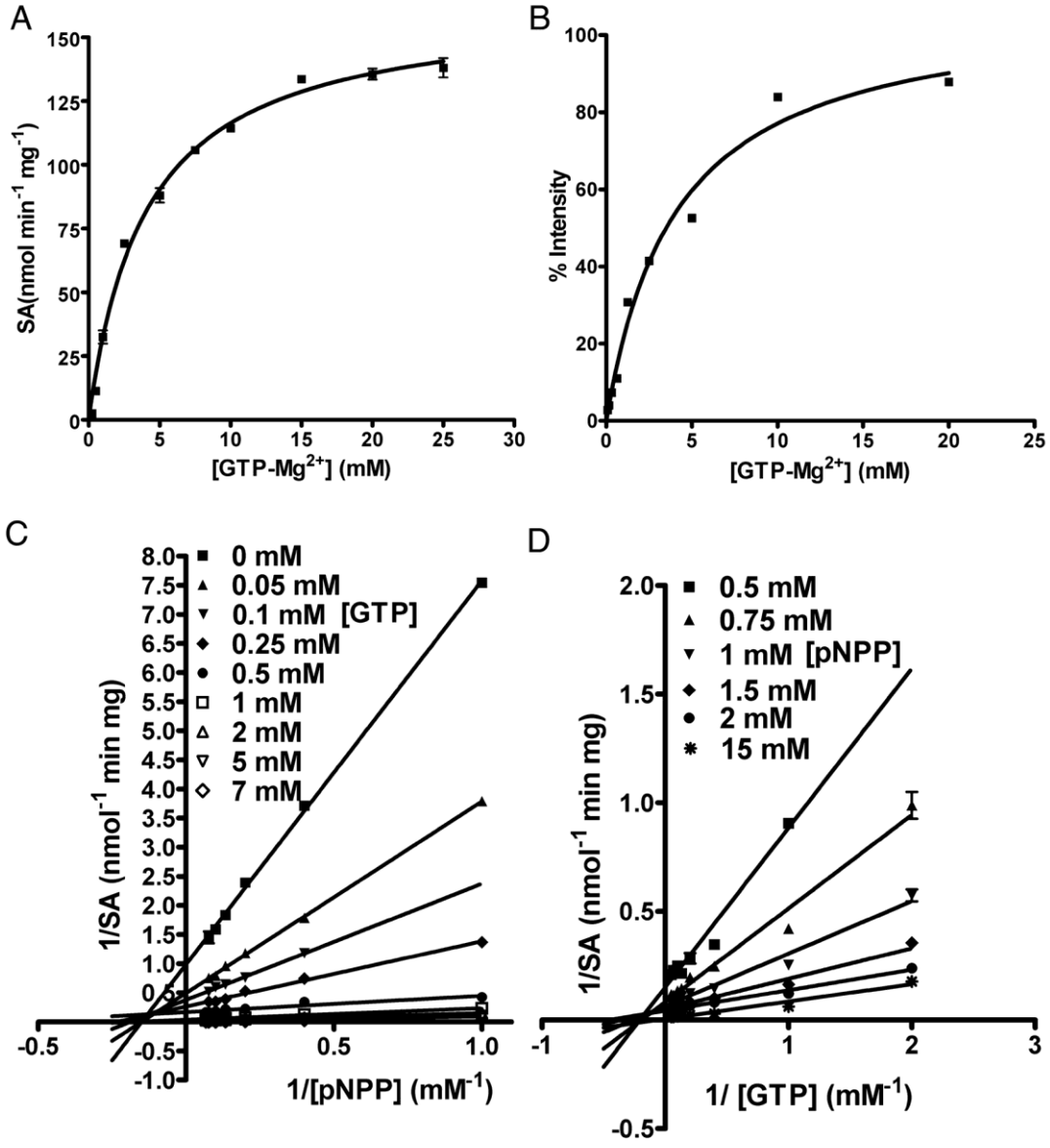

Figure S3. Modulation of GTP activation by various ligands.

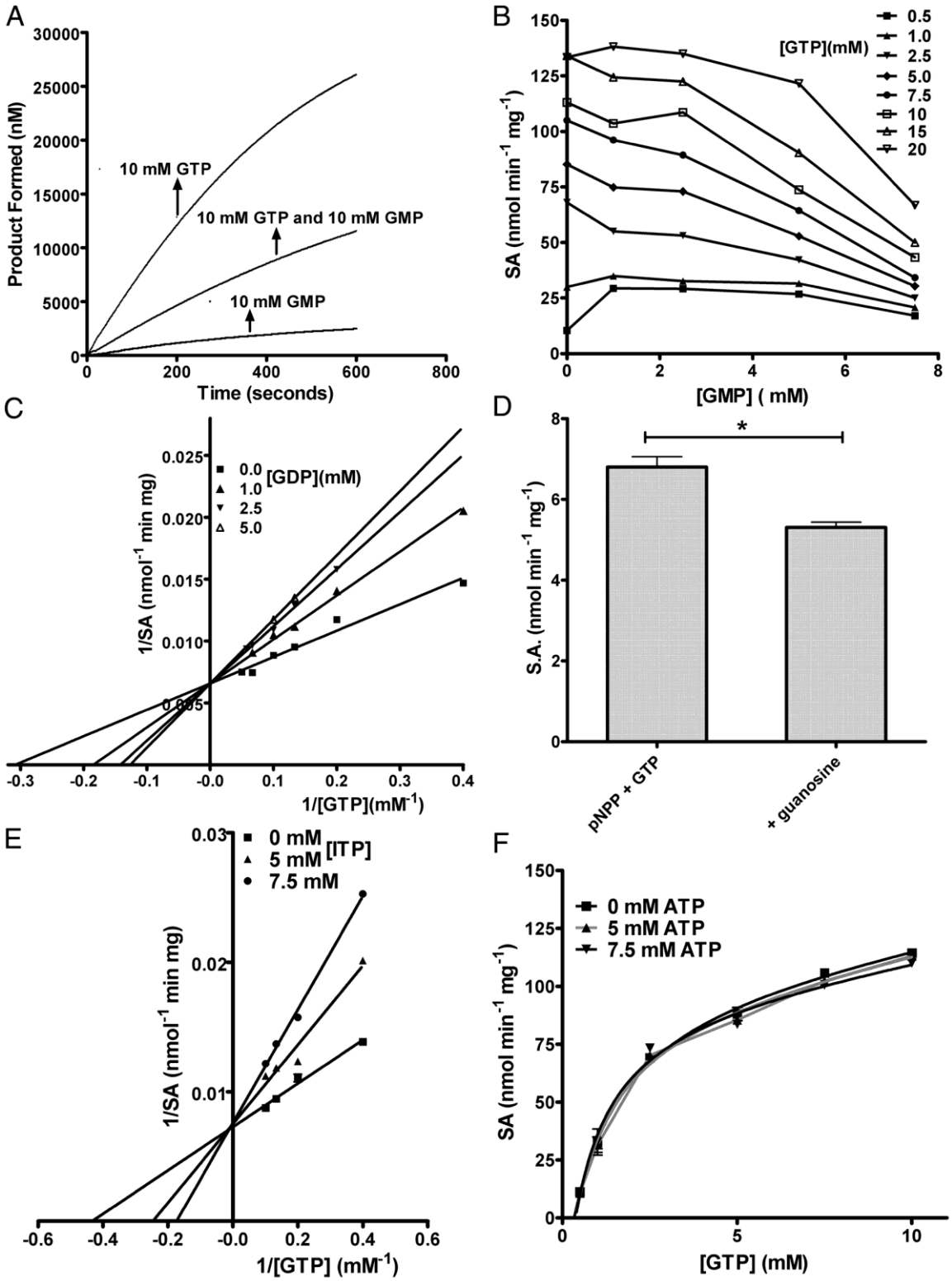

Figure S4. Purification and characterization of LpcN-II mutants.

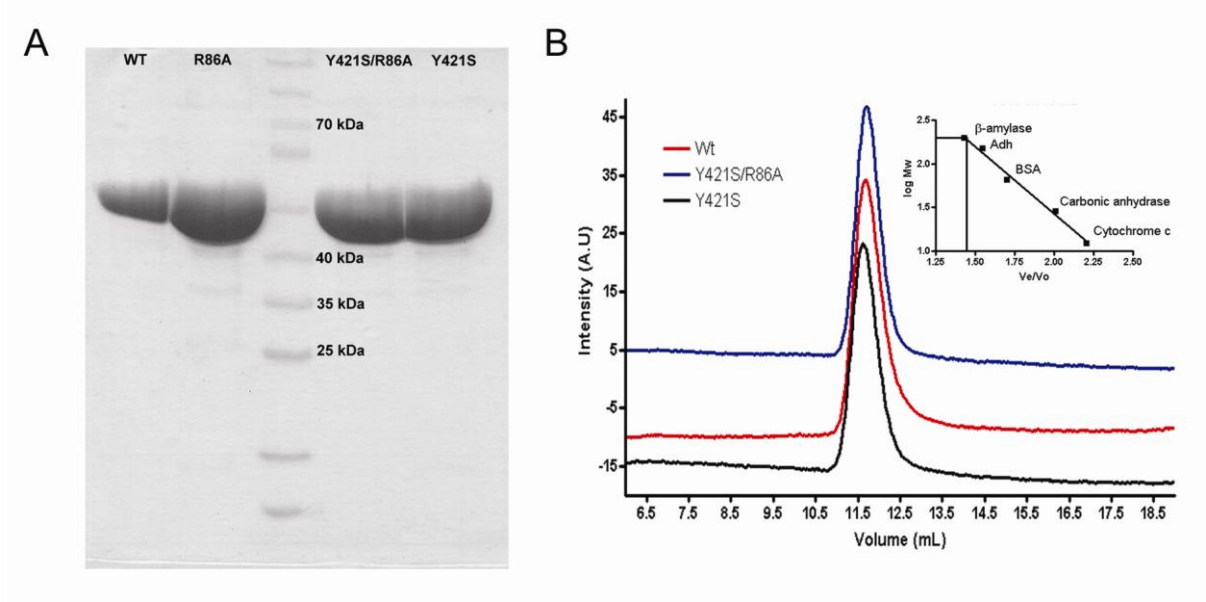

Figure S5. Active site-allosteric site connectivity.

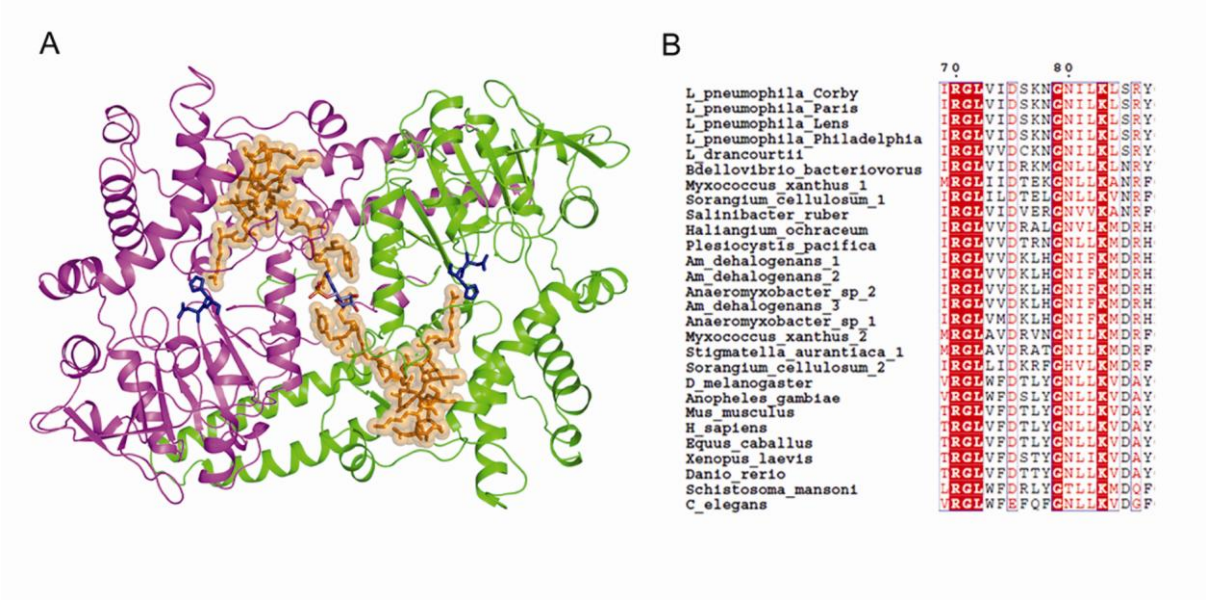

Figure S6. Phylogenetic tree and multiple sequence alignment of cN-IIs from different organisms.